Modeling the Joint Probability Distribution of Main Shock and Aftershock Spectral Accelerations

Sheng Hu
PhD Student, Dept. of Civil and Environmental Engineering, University of Illinois at Urbana-Champaign, Urbana, IL, USA

Armin Tabandeh
Postdoctoral Researcher, Dept. of Civil and Environmental Engineering, University of Illinois at Urbana-Champaign, Urbana, IL, USA

Paolo Gardoni
Professor, Dept. of Civil and Environmental Engineering, University of Illinois at Urbana-Champaign, Urbana, IL, USA

ABSTRACT: Seismic risk analysis of deteriorating structures and infrastructure often requires predicting the intensity measures of earthquake ground motions in main shock-aftershock sequences. The uncertainty in the intensity measures of ground motions is typically a dominant contributor to the total uncertainty of the seismic risk analysis. A model for the joint probability distribution of main shock and aftershock intensity measures is thus required to accurately quantify the uncertainty in the seismic risk analysis. The spectral accelerations of ground motions have been identified as significant intensity measures for the seismic risk analysis of structures and infrastructure. The values of spectral accelerations can be affected by many factors representing the characteristics of the seismic source, travel path of seismic waves, and local site conditions. These factors can also introduce statistical dependence among main shock and aftershock spectral accelerations. This paper develops a novel formulation for the joint probability distribution of main shock and aftershock spectral accelerations at multiple periods. We select existing predictive models for the spectral accelerations of main shocks and develop a separate model for the spectral accelerations of aftershocks. The proposed formulation also estimates the correlations between the relevant pairs of model error terms in the two probabilistic predictive models for a wide range of periods. This allows us to separately capture the similarity in source and site and thus present the physical meanings. The increased vulnerability of structures and infrastructure in the aftermath of a damaging mainshock can further highlight the significance of capturing such correlations in the seismic risk analysis.

1. INTRODUCTION

Seismic risk analysis of deteriorating structures and infrastructure often requires predicting the intensity measures of earthquake ground motions in main shock-aftershock (MS-AS) sequences. Main shocks are typically followed by a sequence of aftershocks of varying magnitudes and with relatively high rates of occurrence that gradually decay over time (Shokrabadi and Burton 2018). Structures can collapse in a small aftershock due to the accumulation of damage from previous main shock and aftershocks. The increased vulnerability of structures and infrastructure in the aftermath of a damaging main shock highlights the significance of modeling the hazard due to MS-AS sequences (Yeo and Cornell 2005; Kumar and Gardoni 2012). Therefore, seismic risk analysis of deteriorating structures and infrastructure need to consider the impact from MS-AS sequences. Spectral accelerations have been identified as significant intensity measures (Gardoni et al. 2003). However, there are not enough spectral accelerations from recorded MS-AS sequences for many structural design scenarios. In addition, the available records are always not complete and may have missing records for aftershocks of considerable intensity. Therefore, using only the limited real ground motions may underestimate the damage to the structures and cannot accurately capture the embedded uncertainty. There is thus a need of a model for generating synthetic sequences of the MS-AS spectral accelerations. The uncertainty in the spectral accelerations is typically a dominant contributor to the total uncertainty in the seismic risk analysis. Other than the marginal variances of MS-AS spectral accelerations, correlation between spectral accelerations of a main shock and its corresponding aftershocks can also have a significant effect (Yeo and Cornell 2005). The uncertainty, including the dependence among MS-AS spectral accelerations can be formulated in a joint distribution. The joint distribution needs to take account for the correlation of spectral accelerations at multiple periods. This is because with the accumulation of damage, the natural period of the structure might change subject to MS-AS sequences.

Ground Motion Prediction Equations (GMPEs) are convenient tools to model the spectral accelerations of earthquake ground motions in MS-AS sequences. Many researchers studied the marginal probability distributions of spectral accelerations for main shock and some of them also studied those for aftershocks. For example, Abrahamson et al. (2013) developed GMPEs that predict the marginal means and standard deviations of the logarithm of spectral accelerations for both main shocks and aftershocks. Only few models have been developed that can capture the statistical dependence of MS-AS spectral accelerations. Most recently, Zhu et al. (2017) developed a model for the correlation between the spectral accelerations of a main shock and its aftershocks but their study was limited to spectral accelerations at the same period. Also, their model only captured the correlation between spectral accelerations of a main shock and its aftershock with the largest magnitude; thus, is not capable of presenting the impact of the complete MS-AS sequence. Furthermore, while using GMPEs to calculate residuals, their model ignored the hierarchical structure of the residuals in the GMPEs and thus calculated the correlation using unbalanced data. This can in turn introduce bias in the correlation coefficient results.

This paper proposes a model for the joint distribution of spectral accelerations at different periods in a MS-AS sequence instead of at the same period. Our model separately uses a two-residual mixed-effect model as in NGA-West2 project for main shocks and a novel three-residual mixed-effect model for aftershocks. By modeling the correlation of two pairs of residuals from the two mixed-effect model, we reduce the bias caused by the unbalanced data. The two pairs of residuals each represent the similarities in terms of the site condition and seismic source between MS-AS spectral accelerations. The model is then calibrated using recorded main shock and aftershock ground motions. We also present an approach to simulate synthetic MS-AS sequences of spectral accelerations at different periods using the developed joint distribution model.

2. MODEL FOR THE JOINT DISTRIBUTION OF SPECTRAL ACCELERATIONS

2.1. General approach

The joint distribution of spectral accelerations depends on the associated earthquake characteristics and site conditions. For example, for spectral accelerations at different periods for the same ground motion, the source, seismic wave path, and site conditions are the same, which could have similar effects on the spectral accelerations. Therefore, the correlation between the spectral accelerations is expected to be relatively higher than spectral accelerations in different ground motions. For main shock and aftershocks in the same sequence, the magnitude of the aftershocks are positively correlated with the corresponding main shock's magnitude (Shcherbakov and Turcotte 2004). Aftershocks are likely to occur close to the main shock source and on the same fault; thus, the seismic wave path and source characteristics of the main shock and its aftershocks is also expected to be correlated. These factors can significantly affect the correlations among spectral accelerations in a MS-AS sequence; thus, we use parametric models using the earthquake characteristics as predictors in our modeling of the statistical dependence. In this paper, we use two separate parametric models for the means of main shock and aftershock spectral accelerations conditioned on their associated earthquake characteristics and site conditions. We also estimate the correlation between pairs of unexplained residuals.

2.2. Model for main shock spectral accelerations

Existing GMPEs (e.g., Abrahamson et al. 2013; Campbell and Bozorgnia 2014) can provide the marginal distributions of spectral accelerations at a range of periods. The prediction equations for the spectral accelerations are fitted at different periods and use different sets of predictors. We select the ASK14 (Abrahamson et al. 2013) and the CB14 (Campbell and Bozorgnia 2014) models as our main shock models in this study. Both models are part of the results of the NGA-West 2 Project and we select two of them so that we can compare the results and examine the effect of using different parametric models. The form of the prediction equation is as follows:

$$v_{i,j0l} = \mu_i(\mathbf{x}_{i,j0l}, \boldsymbol{\theta}_{i0}) + \kappa_{i,j0} + \varepsilon_{i,j0l} \qquad (1)$$

where $v_{i,j0l}$ is the logarithm of the spectral acceleration at the ith period, for the lth record from the jth main shock; subscript "0" is the index for mainshocks; $\mu_i(\cdot)$ is the mean function; $\mathbf{x}_{i,j0l}$ and $\boldsymbol{\theta}_{i0}$ are predictors and model parameters; $\kappa_{i,j0}$ and $\varepsilon_{i,j0l}$ are the inter-event and intra-event residuals, in which $\kappa_{i,j0}$ captures the effects of the seismic source and $\varepsilon_{i,j0l}$ captures the effects of site conditions, seismic wave paths, and unexplained noise for different records at different stations for the same event. Both residuals are independent random variables from each other and from the predictors.

2.3. Model for aftershock spectral accelerations

Some GMPEs are also available for spectral accelerations of aftershocks (e.g., Abrahamson et al. 2013). Such models were developed to include the different features of aftershocks (Boore and Atkinson 1992; Goda and Taylor 2012). Hu et al. (2018) developed a procedure to simulate synthetic main shock-aftershock ground motion sequences. While predicting some key features for ground motions, they added a special random effect term, inter-sequence residual, to represent the difference across MS-AS sequences. Likewise, we develop three-residual GMPEs for aftershocks in the following form:

$$v_{i,jkg} = \mu_i(\mathbf{x}_{i,jkg}, \boldsymbol{\theta}_{i1}) + \kappa_{i,j} + \gamma_{i,jk} + \varepsilon_{i,jkg} \qquad (2)$$

where $v_{i,jkg}$ is the logarithm of the spectral acceleration at the ith period, for the gth record from the kth earthquake in the jth sequence; subscript $k > 0$ is the index for aftershocks; $\mathbf{x}_{i,jkg}$ and $\boldsymbol{\theta}_{i1}$ are predictors and model parameters; $\kappa_{i,j}$, $\gamma_{i,jk}$ and $\varepsilon_{i,jkg}$ are the inter-sequence, inter-event and intra-event residuals, respectively. While the intra-event residuals model similar effects as in the main shock model, the inter-sequence residuals capture the common source effects of the events in the same sequence. Furthermore, the inter-event residual now captures the different effects of events in the same sequence as well as the common source effect in the same event. When calculating the correlation of residuals, the inter-sequence residual could conveniently correspond to the inter-event residual in the main shock model, which captures the effect of the main shock source. The three residuals in Equation (2) are independent random variables from each other and from the predictors.

2.4. Correlation model for main shock residuals and aftershock residuals

Using the models in Eqs. (3) and (4) for the spectral accelerations of main shocks and aftershocks, we can write

$$[v_{i,j0l} - \mu_i(\mathbf{x}_{i,j0l}, \boldsymbol{\theta}_{i0}),\\ v_{i,jkg} - \mu_i(\mathbf{x}_{i,jkg}, \boldsymbol{\theta}_{i1})] \quad (3)\\ \equiv [\kappa_{i,j0} + \varepsilon_{i,j0l}, \kappa_{i,j} + \gamma_{i,jk} + \varepsilon_{i,jkg}]$$

Among the residuals in the two models, both $\kappa_{i,j0}$ and $\kappa_{i,j}$ capture the effects of the source on spectral accelerations and both $\varepsilon_{i,j0l}$ and $\varepsilon_{i,jkg}$ capture the effects of site conditions and seismic wave paths at the same recording station. We model the correlations for the pairs $(\kappa_{i,j0}, \kappa_{i,j})$ and $(\varepsilon_{i,j0l}, \varepsilon_{i,jkg})$ and assume that other residuals at different levels of the hierarchy can be simulated independently across the two models.

2.5. Specification of the type of the joint distribution

Multivariate normality is often assumed for the logarithm of spectral accelerations at different periods (Jayaram and Baker 2008). Therefore, we take the multivariate normal distribution as the hypothesis and use statistical methods to examine its validity. Other distributions (e.g., Generalized Extreme Value) will be taken into consideration only when the multivariate normality is rejected.

3. CALIBRATION OF THE JOINT DISTRIBUTION MODEL

3.1. Ground motion database

We select main shock and aftershock ground motions from the NGA-West2 Database (Ancheta et al. 2014) to calibrate the joint distribution of the spectral accelerations for main shocks and aftershocks. Therefore, our model focuses on shallow crustal earthquakes in active tectonic regions. The database provides characteristics of each earthquake, site conditions at each recording stations as well as the classification to main shocks or aftershocks for each recorded seismic event. Following the criteria proposed in Abrahamson et al. (2013), we collect 14016 available ground motions from 241 events classified as main shocks. Following the criteria proposed in Campbell and Bozorgnia (2014), we collect 14366 main shock ground motions from 320 events classified as main shocks. The NGA-West2 Database used the Centroid Joyner-Boore distance (CR_{jb}) to classify main shock and aftershocks. The distance measure CR_{jb} is the shortest distance from the centroid point of the Joyner-Boore rupture surface of one potential aftershock to the closest point on the edge of the Joyner-Boore rupture surface of the main shock. To measure the effect of the distance between main shock source and aftershock source on spectral accelerations, we use the threshold of 40 km for the classification. We collect 2816 aftershock ground motions from 131 events classified as aftershocks.

PEER NGA-West2 database (Ancheta et al. 2014) processed each of its ground motions using a high-pass filter and a low-pass filter. Therefore, in the calibration process we exclude those spectral accelerations at periods higher than their low-pass filter and lower than their minimum usable period provided by NGA-West2 database.

3.2. Available Predictors

Based on the knowledge of potential faults and regional seismicity, we can simulate sequences of characteristics including fault mechanism, occurrence time, source location and magnitude (e.g. Turcotte et al. 2007). Therefore, the joint distribution of spectral accelerations in a MS-AS sequence can be conditioned on the given earthquake characteristics at each sampling step. In this paper, we assume the knowledge of the magnitude, hypocenter location, and a defined finite rupture model for the main shock. We also assume the knowledge of magnitudes, epicenter locations for the aftershocks, and the knowledge of shear-wave velocity over the top 30 m of the subsurface profile, V_{s30}, at the site for the recording station. According to the availability of information, one may select different parametric models in Sections 3.3 and 3.4.

3.3. Estimation of main shock inter-event and intra-event residuals

Both ASK14 and CB14 GMPEs provide spectral accelerations at 21 different periods spanning $[0.01s, 10s]$. For each of the main shock ground motions collected in our database, we predict the mean and standard deviations using the spreadsheet developed by the PEER NGA-West2 Group. We can obtain the total residuals as

$$\delta_{i,j0l} = \ln Sa_{i,j0l} - \mu_{\ln Sa_{i,j0l}} \quad (4)$$

where $\delta_{i,j0l}$ is the total residual for the lth record of the jth main shock at the ith period; $\mu_{ln\, Sa_{i,j0l}}$ is the corresponding predicted mean from a GMPE; $Sa_{i,j0l}$ is the spectral acceleration of the corresponding recorded ground motion at the ith period. We then separate the total residuals to inter-event residuals and intra-event residuals by fitting a random-effect model as

$$\delta_{i,j0l} = \hat{\kappa}_{i,j0} + \hat{\varepsilon}_{i,j0l} \quad (5)$$

where $\hat{\kappa}_{i,j0}$ and $\hat{\varepsilon}_{i,j0l}$ are the estimates of $\kappa_{i,j0}$ and $\varepsilon_{i,j0l}$ calibrated in Abrahamson et al. (2013). Due to the varying low-pass filter frequency and high-pass filter frequency, we have varying number of supports, the number of data points used to calibrate the prediction equations, at different periods. Other than spectral accelerations at 0.01s, for which there is no data for the calibration, the least support is 462 using the ASK14 model and 512 using the CB14 model. We calibrate the prediction equations at different periods independently. We then use Q-Q plots to examine the normality of the predicted residuals. The estimated correlations for the pairs $(\kappa_{i,j0}, \kappa_{i\prime,j0})$ and $(\varepsilon_{i,j0l}, \varepsilon_{i\prime,j0l})$, namely the residuals at different periods in the same record, using ASK14 model are similar to those reported in (Abrahamson et al. 2013).

3.4. Estimation of aftershock inter-sequence, inter-event and intra-event residuals

We select 111 periods spanning $[0.01s, 10s]$. Other than spectral accelerations at 0.01s, for which there is no data for the calibration, the least support is 269. We calibrate the prediction equations at different periods independently.

We consider a wide range of candidate predictors. We choose the candidate predictors mostly according to the ground motion prediction equations (GMPEs) already developed as a part of the NGA-West2 Project. The candidate predictors capture the effects of fault mechanism (reverse, normal, strike-slip), magnitude, path, site condition, relative location of the aftershock source to its corresponding main shock source, and time interval of the aftershock and its corresponding main shock. To avoid the possible computational difficulties from largely differed scales of predictors when estimating the regression coefficients, we made dimensionless the predictors other than those representing fault mechanisms, by dividing the actual values by a typical value of the predictor.

We use the p-values reported by R-package “lmerTest” (Kuznetsova et al. 2017) as a measure of the significance of a predictor, which is based on denominator degrees of freedom computed using Satterthwaite’s method (Satterthwaite 1946). We manually add or remove a predictor until all the predictors become significant at multiple periods spanning from 0.01 to 10 sec. Despite some close exceptions (at several periods, p-values for a predictor is right below 0.05 but all other p-values are as small as $2e - 16$), we could select a uniform set of predictors for all periods. The selected predictors are

$$\boldsymbol{Z} = [M_{\mathrm{W}}, M_{\mathrm{W}} \cdot \ln \sqrt{R_{\mathrm{Rup}}^2 + h^2}, V_{\mathrm{s30}}] \quad (6)$$

where M_{W} is the moment magnitude; R_{Rup} is the rupture distance, which is the closest distance from the recording site to the ruptured area; h is set to 3.5 km according to the estimates given in Abrahamson et al. (2013).

3.5. Estimation of correlation coefficients

We select the Pearson product-moment correlation coefficient as a measure for the correlation of the residual pairs $(\kappa_{i,j0}, \kappa_{i,j})$ and $(\varepsilon_{i,j0l}, \varepsilon_{i,jkg})$, which is defined as

$$\hat{\rho}_{X,Y} = \frac{\sum_{q=1}^{n}(X_q - \bar{X})(Y_q - \bar{Y})}{\sqrt{\sum_{i=1}^{n}(X_q - \bar{X})^2 \sum_{i=1}^{n}(Y_q - \bar{Y})^2}} \quad (7)$$

where X_q and Y_q are the qth pair of observed values of random variables X and Y; $\bar{X}$ and $\bar{Y}$ are the sample means of X and Y.

3.5.1. Main shock inter-event residuals and aftershock inter-sequence residuals

As discussed previously in this section, the corresponding main shock and aftershock records may have different high-pass and low-pass filter frequencies. Also, due to limited available data, we calibrate the main shock model and the aftershock model with records from different sets of sequences. Therefore, at each period, we need to pair the main shock inter-event residuals and the aftershock inter-sequence residuals corresponding to the same sequences. Figure 1 shows the estimated correlation between inter-event residuals of main shocks and their aftershocks. We calculate the correlation of main shock inter-event residuals at 21 periods (using CB14 model, the ASK14 model show similar results) and aftershock inter-sequence residuals at 111 periods and plot them as solid-line contour. The dash-line contour represents the range where the number of supporting pairs of residuals is larger than 25 (the larger box) and 30 (the smaller box). We can observe that for the period of the spectral acceleration of the main shock varying in the range $[0.05s, 1s]$, the correlation varies from $+0.4$ to -0.1 as the period of the aftershock spectral acceleration changes from 0.1s to 1s. The correlation of inter-event residuals depends on the value of the period for aftershock spectral accelerations more than on the interval of the periods for the corresponding main shock and aftershock spectral accelerations. The database we use in this paper is sufficient to estimate the correlation for main shock and aftershock spectral accelerations falling in the period range of approximately 0.05s to 3s (with support larger than 25).

3.5.2. Main shock intra-event residuals and aftershock intra-event residuals

Similar to the approach we use in Section 3.5.1, at each period, we pair the main shock intra-event residuals and the aftershock intra-event residuals corresponding to the same station and calculate their correlation. We show the calculation results as solid-line contour in Figure 2. The dash-line box represents the range where the number of supporting pairs of residuals is larger than 1500. We can observe that the most significant correlation between the intra-event residuals can be as significant as 0.4 along the diagonal line where the periods are equal for the main shock spectral accelerations and the aftershock spectral accelerations. The correlation vanishes as the difference of periods gets larger. The database we used in this paper is sufficient to estimate the correlation for main shock and aftershock spectral accelerations over the period range 0.02s to 10s (with support larger than 25).

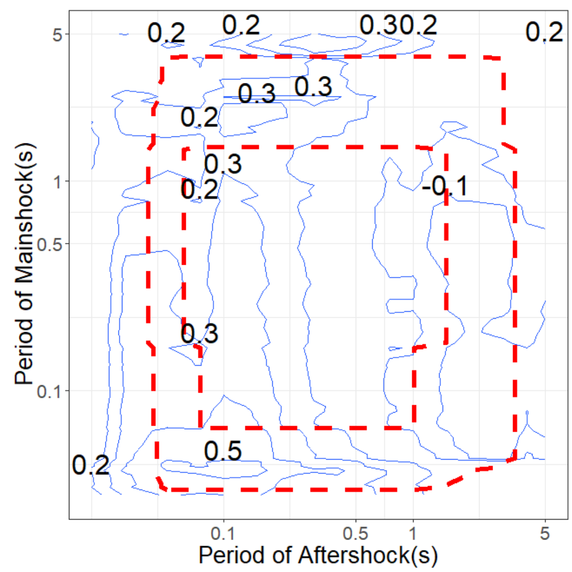

Figure 1 Correlation contour for main shock inter-event residuals (CB14) and aftershock inter-sequence residuals

3.6. Specification of the type of the joint distribution

We use an R package "MVN" (Korkmaz et al. 2014) to examine the hypothesis of multivariate normality. The package provides five normality tests ("hzTest" "mardiaTest", "roystonTest", "Energy" and "dz").

For the joint distribution of the main shock inter-event residuals and aftershock inter-sequence residuals, except for rare exceptions on data points of low supports, bi-variate normality assumptions for the pairs of residuals at all main shock periods and all aftershock periods cannot be rejected. We further conduct multivariate normality check on up to three main shock periods along with up to three aftershock periods, multivariate normality holds in multiple combinations of periods with few exceptions.

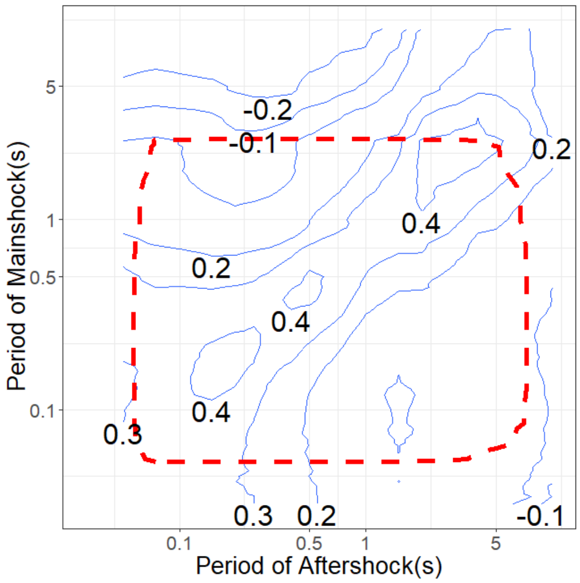

Figure 2 Correlation contour for main shock intra-event residuals (CB14) and aftershock intra-event residuals

For the joint distribution of the main shock intra-event residuals and aftershock intra-event residuals, using all pairs of available data in one test is not appropriate. This is because one main shock record may correspond to several aftershock records in the same sequence, which results in repeated use of main shock residuals. Following Jayaram and Baker (2008), we examine the multivariate normality using pairs of residuals from a single pair of main shock and aftershock events. Among the examined main shock-aftershock pairs, only three aftershocks in the Chi-Chi earthquake sequence strongly violate the multivariate normality assumption. This may be caused by the strong spatial correlation between closely located stations. To avoid the strong correlation between neighboring stations in these well-recorded earthquake events, we selected only part of the data points so that they are at least 0.1° in latitude or longitude away from each other. We also normalized both sets of residuals to avoid the effect of the bias in the marginal distribution (since the normality of the marginal distributions are already examined). The multivariate normality hypothesis for the selected and processed pairs of residuals cannot be rejected for the three aftershocks.

4. SIMULATION OF SPECTRAL ACCELERATIONS USING THE JOINT DISTRIBUTION

When used to evaluate the structural performance, spectral accelerations can be sampled one-by-one at varying natural periods of the studied structures as damage accumulates when subjecting to the MS-AS sequence. To start with, the spectral acceleration of the main shock may be sampled from $f_0(v_0)$, which represents an existing model of the marginal distribution of v_0. In this paper, v_0 represents $\log Sa_0(T_0^-)$, the logarithm of the spectral acceleration of the main shock ground motion at T_0^-, the natural period of the studied structure before the main shock. We may sample the spectral acceleration of the ith aftershock from the following conditional distribution:

$$f_{i|\boldsymbol{P}}(v_i|\boldsymbol{v_P}) = \frac{f_{i\boldsymbol{P}}(v_i,\ \boldsymbol{v_P})}{f_{\boldsymbol{P}}(\ \boldsymbol{v_P})} \tag{8}$$

where $\boldsymbol{v_P} = [v_0, v_1, \dots, v_{i-1}]$ is the vector of logarithm of spectral accelerations of the main shock and all aftershocks before the ith one; and $f_{i\boldsymbol{P}}(v_i, \boldsymbol{v_P})$ is the joint distribution of v_i and $\boldsymbol{v_P}$. As discussed in Section 3.6, $f_{i|\boldsymbol{P}}(v_i|\boldsymbol{v_P})$ is a conditional normal probability distribution function with mean and variance that can be calculated using the models and correlations calibrated in Section 3.

5. CONCLUSIONS

This paper proposed a formulation for the joint distribution of main shock and aftershock spectral accelerations. The formulation consists of separate parametric models for main shocks and aftershocks and estimated correlations between pairs of unexplained residuals. The common effect of similar source characteristics of an aftershock and its main shock is captured by the correlation of the inter-event residual in the main shock model and inter-sequence residual in the aftershock model. Furthermore, the common effect of similar site conditions for two ground motions recorded at the same station is captured by the correlation between the intra-event residual in the main shock model and the intra-event residual in the aftershock model. We calculated the correlations between the two pairs of the residuals of spectral accelerations at the same or different periods. The multivariate normality of these two pairs of residuals are examined and no strong evidence is observed to reject the assumption. The main shock model, the aftershock model, and the estimated correlation can therefore describe the joint distribution of main shock and aftershock spectral accelerations at multiple periods. The developed models can be used to simulate main shock-aftershock sequences of spectral accelerations at the same site.

6. REFERENCES

Abrahamson, N. A., Silva, W., and Kamai, R. (2013). "Update of the AS08 Ground-Motion Prediction equations based on the NGA-west2 data set." *PEER Report 2013/04*, Pacific Earthquake Engineering Research Center, Berkeley, CA.

Ancheta, T. D., Darragh, R. B., and Stewart, J. P. (2014). "PEER NGA-West2 Database." *Earthquake Spectra*, 30(3), 989–1005.

Boore, D. M., and Atkinson, G. M. (1992). "Source spectra for the 1988 Saguenay, Quebec, earthquakes." *Bulletin of the Seismological Society of America*, 82(2), 683–719.

Campbell, K. W., and Bozorgnia, Y. (2014). "NGA-West2 ground motion model for the average horizontal components of PGA, PGV, and 5% damped linear acceleration response spectra." *Earthquake Spectra*, 30(3), 1087–1114.

Gardoni, P., Mosalam, K. M., and Kiureghian, A. D. E. R. (2003). "Probabilistic seismic demand models and fragility estimates for RC bridges." *Journal of Earthquake Engineering*, Taylor & Francis, 7(sup001), 79–106.

Goda, K., and Taylor, C. A. (2012). "Effects of aftershocks on peak ductility demand due to strong ground motion records from shallow crustal earthquakes." *Earthquake Engineering and Structural Dynamics*, 41(15), 2311–2330.

Hu, S., Gardoni, P., and Xu, L. (2018). "Stochastic procedure for the simulation of synthetic main shock-aftershock ground motion sequences." *Earthquake Engineering and Structural Dynamics*, 47(11), 2275–2296.

Jayaram, N., and Baker, J. W. (2008). "Statistical tests of the joint distribution of spectral acceleration values." *Bulletin of the Seismological Society of America*, 98(5), 2231–2243.

Korkmaz, S., Goksuluk, D., and Zararsiz, G. (2014). "MVN: An R package for assessing multivariate normality." *The R Journal*, 6(2), 151–162.

Kumar, R., and Gardoni, P. (2012). "Modeling Structural Degradation of RC Bridge Columns Subjected to Earthquakes and Their Fragility Estimates." *Journal of Structural Engineering*, 138(1), 42–51.

Kuznetsova, A., Brockhoff, P., and Christensen, R. (2017). "lmerTest Package: Tests in Linear Mixed Effects Models." *Journal of Statistical Software*, 82(13), 1–26.

Satterthwaite, F. E. (1946). "An Approximate Distribution of Estimates of Variance Components." *Biometrics Bulletin*, 2(6), 110.

Shcherbakov, R., and Turcotte, D. L. (2004). "A modified form of Båth's law." *Bulletin of the Seismological Society of America*, 94(5), 1968–1975.

Shokrabadi, M., and Burton, H. V. (2018). "Risk-based assessment of aftershock and mainshock-aftershock seismic performance of reinforced concrete frames." *Structural Safety*, Elsevier, 73(March), 64–74.

Turcotte, D. L., Holliday, J. R., and Rundle, J. B. (2007). "BASS, an alternative to ETAS." *Geophysical Research Letters*, 34(12), 1–5.

Yeo, G. L., and Cornell, C. A. (2005). "Stochastic Characterization and Decision Bases under Time-Dependent Aftershock Risk in Performance-Based Earthquake Engineering." *PEER Report 2005/13*, Pacific Earthquake Enginnering Research Center.

Zhu, R. G., Lu, D. G., Yu, X. H., and Wang, G. Y. (2017). "Conditional mean spectrum of aftershocks." *Bulletin of the Seismological Society of America*, 107(4), 1940–1953.